

AN ANALYSIS OF THE IMPLOSION OF HEAVY ION DIRECTLY DRIVEN SIMPLE TARGETS

G. VELARDE, J. M. MARTINEZ-VAL, C. GONZÁLEZ, M. PIERA,
J. M. ARAGONÉS, L. GÁMEZ, J. J. HONRUBÍA, E. MÍNGUEZ,
J. M. PERLADO, and P. M. VELARDE

Institute of Nuclear Fusion, Denim J. Gutiérrez Abascal, 2. 28006 Madrid, Spain.

(Received 3 December 1990)

Hollow targets made of a lithium-coated shell of DT are considered. This type of simple target is selected to try to avoid hydrodynamic instabilities. The last phase of the implosion process is particularly analyzed. It is found that ignition can be achieved if fuel stagnation is avoided. Stagnation can appear if the fuel is unsuitably accelerated during the compression phase and the innermost layer of fuel reaches a speed much higher than the speeds of the outer layers. The main parameter governing the fuel acceleration is the dose rate delivered in the lithium by the driving pulse. Neither pulse shaping nor voltage ramping is necessary. Numerical simulations show that energy gains above 50 can be obtained with 1-mg DT targets and 2 to 3 MJ of driving pulse.

1 INTRODUCTION AND SCOPE OF THE PAPER

Heavy ion direct drive requires very uniform target illumination, which seems to be a condition very difficult to meet with the standard focusing technology. Nevertheless, the theoretical value of this concept has guided important studies, as the HIBALL conceptual design¹, and deserves a deep investigation to identify the ranges of variables yielding optimum performance. Several important papers have been published regarding this analysis^{2–8}.

This article is intended to analyze, by numerical simulation, a given type of targets made of a shell of DT surrounded by a thick coating of lithium. Such a simple target is devised to avoid strong density gradients that can induce destructive mixing through hydroinstabilities. The numerical analysis was carried out with the NORCLA computer code, which has been applied in several Inertial Confinement Fusion studies^{9–11}. Former calculations⁸ had shown that high energy gains, close to 100, could be obtained with multilayered single-shell targets (HIBALL-type) of 1 mg DT, driven by Bi⁺ beams of 2 MJ, using voltage ramping in order to compensate the ion range shortening. Nevertheless, that result could be considered too optimistic because the density jump across the lead-fuel interface was extremely high and Rayleigh-Taylor mixing could happen just after the central void closure.

In this paper, Bi⁺ ions are also used as driving beams. A parametric study has been carried out, the ranges of variation being as follows: accelerating voltage, from

1 GV up to 10; beam power, from 100 TW up to 500 TW; pulse length, from 8 to 20 ns; total energy, from 1 MJ to 5 MJ; and fuel aspect ratio (A.R.), from 50 to 100. The lithium coating thickness was fixed at 20% larger than the initial ion range in cold lithium. Some important conclusions have been drawn from this study.

2 BEAM ENERGY DEPOSITION AND FUEL ACCELERATION

Besides the stopping mechanisms by cold matter, our numerical simulation takes into account the contribution to the stopping power by ions and, mainly, free electrons. The equilibrium effective charge of the incoming Bi ions at each calculation step is taken into account. Hence, range shortening modifies the profile of energy deposition vs. time.

Temperatures achieved in the lithium depend mainly on the dose rate i.e., the energy deposited per mass and time unit. As the lithium mass of the target is much lower for 1 GeV ions than for 10 GeV ions, the dose rate increases as the voltage decreases, and lithium temperatures can reach 100 eV in 1 GeV-driven targets. Marshack waves can develop inwards, so preheating the fuel and hampering compression. In a 2 MJ, 200 TW, 1 GeV case, the bulk of the fuel arrived at 25 eV before void closure, and the target performance was rather poor. Moreover, strong shock waves emerging from the high-pressure zone of the lithium coating induced a very non-uniform acceleration of the fuel, the innermost part of it flying much faster than the bulk towards the center. The importance of this fact will be emphasized later on. For our first numerical survey, the accelerating voltage was limited to 6–10 GV in order to induce a proper fuel implosion.

The compression in this phase follows an almost adiabatic evolution, with a γ about 1.7, but the innermost part of the fuel is in a higher adiabatic state than the

TABLE 1
Evolution of Energy Magnitudes in a target Driven by 10 GeV Bi⁺ Ions, 200 TW, 15 ns Pulse (all Variables in MJ).

t (ns)	Ablation energy	Kinetic E. of lithium (inward)	Kinetic E. of DT (inward)	Internal energy of lithium	Internal energy of DT
1	0.00025	0.0003	0.00001	0.198	0.0001
5	0.0456	0.0556	0.00117	0.876	0.00022
10	0.300	0.256	0.0095	1.385	0.00026
15	1.006	0.517	0.180	1.389	0.00025
20	1.703	0.596	0.297	0.597	0.00063
22	1.831	0.543	0.0500	0.506	0.00176
22.8	1.865	0.445	0.0436	0.550	0.0108
23.1	1.877	0.284	0.0307	0.629	0.0741
23.2	1.880	0.181	0.0146	0.667	0.1563
23.2	1.884	0.099	0.0035	0.700	0.2290
23.4	1.940	0.067	0.000	0.720	0.1617

outer part. As an example, when crossing the point of $1 \text{ cm}^3/\text{g}$ specific volume, the pressure in the innermost point is 3 terapascals, while that of the outermost point is only 0.2 TPa. This means that the inner point will reach a hotter state than the outer part, though it will not be as dense.

Table 1 shows the evolution of the main energy variables of a target of 1 mg DT (aspect ratio = 100) coated by 376 mg of lithium, illuminated by a pulse of 10 GeV ions at 200 TW over 15 ns. The table reports the pure hydrodynamic calculation without accounting for the energy generated by fusion reactions. As a fraction of the deposited energy arrives to the fuel, it is accelerated towards the center, but it is worth pointing out that the inner part of the lithium conveys a bigger amount of kinetic energy, a fraction of which will be transferred to the compressed fuel, thus increasing the compression performance. The maximum kinetic energy of the mass flying inwards is reached as the void closes, which happens at 22.78 ns in this case. The maximum of fuel internal energy is reached at 23.3 ns, with a ρR of 7 g/cm^2 . It can be seen that more than 7% of the pulse energy is finally transferred to the fuel.

3 THE FINAL STATE OF THE IMPLOSION PROCESS

When the central void collapses, a first hot spark appears, but the fuel compression is still so low that propagation of ignition fails. The total fuel ρR at that time is always lower than 0.2 g/cm^2 . The situation is totally different from laser fusion, where a suitable ignition state can be created at that moment by shock multiplexing¹³. The difference arises from the very different interaction mechanisms between the target and the driving beams. Unlike in laser fusion, where most of the energy is deposited in a very thin region around the critical surface, the energy deposition by ions affects targets of very large volumes that have a mass of a few hundred milligrams.

As the void collapses, the kinetic energy is converted into internal energy according to the energy conservation law. If thermal equilibrium between ions and electrons is assumed, a speed of $8.5 \cdot 10^7 \text{ cm/s}$ is needed to reach 5 keV after void closure. However, ion, electron and radiation temperature begin to separate from this moment on, and the ion temperature will increase significantly faster than the others. That means that it is not necessary to reach the abovementioned speed to trigger ignition.

However, we have already said that such a first hot spark following the void closure is not useful to trigger fusion. At that time, most of the inwards kinetic energy (of the fuel and the internal lithium) has not yet been transferred to fuel internal energy. It will take some time to stop these masses, and the speed profile will play a major role in this deceleration phase. Two different situations can be found:

- If the speed profile is very steep, i.e., the innermost fuel has been accelerated much more than the outermost fuel, the fuel will stagnate. That means that the central overpressure subsequent to the void closure will generate an outgoing shock wave, and the outer fuel will be stopped very far from the center without contributing again to raising the central temperature. Such a situation can be seen in Figure 1, corresponding to a target illuminated by two successive pulses: the first one is made

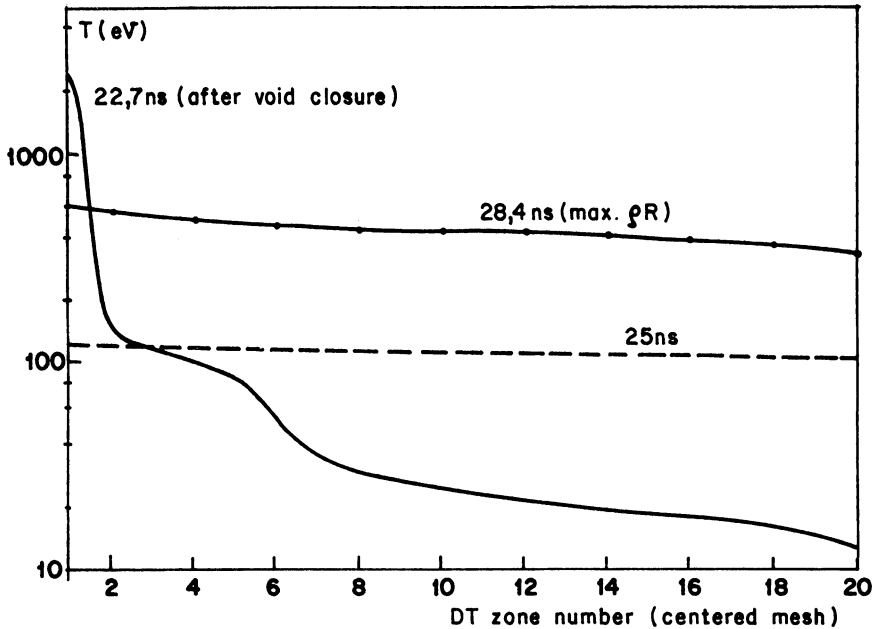


FIGURE 1 Temperature profile evolution after void closure of a target with speed gradient at the end of the flight (see text for case specifications).

of 1.8 GeV ions, 70 TW power, 10 ns length, followed by a main pulse of 6 GeV ions with 140 TW power and 10 ns length, with a total energy of 2.1 MJ. The void closes at 22.7 ns, while the maximum compression is reached at 28.4 ns. The figure depicts how a hot spark is formed after void closure, but 2 ns later the fuel has become almost isothermalized, the outermost part of it still going inwards. The temperature profile at 28.4 ns is also shown. The situation is valid for neither a hot-spark ignition nor volume ignition¹⁴. Such evolution is explained by the speed profile before void closure. The innermost fuel meshpoint (5% of the fuel mass) was flying at $4.7 \cdot 10^7$ cm/s and the fuel-lithium interface at $2.2 \cdot 10^7$ cm/s. This unsuitable speed profile was due to the dual driving pulse, which accelerates the internal fuel much more than the rest.

- The fuel undergoes a very different evolution if the speed profile is fairly uniform. In this case, the delay between void closure and the time of maximum compression is very small (some tenths of a nanosecond) and the final condition is very suitable for initiating ignition. The central temperatures rises to some keV, while the bulk of the fuel is at about 1 keV but at a higher density. There is not fuel stagnation (no isothermalization) and there is not time enough for the outgoing shock wave (subsequent to void closure) to extract energy out from the center and to stop the outer fuel in a position far from it. Of course, the maximum central temperature and the maximum ρR depend on the amount of energy carried by the fuel (and the internal lithium). Figure 2 shows the temperature vs. density evolution of a target illuminated

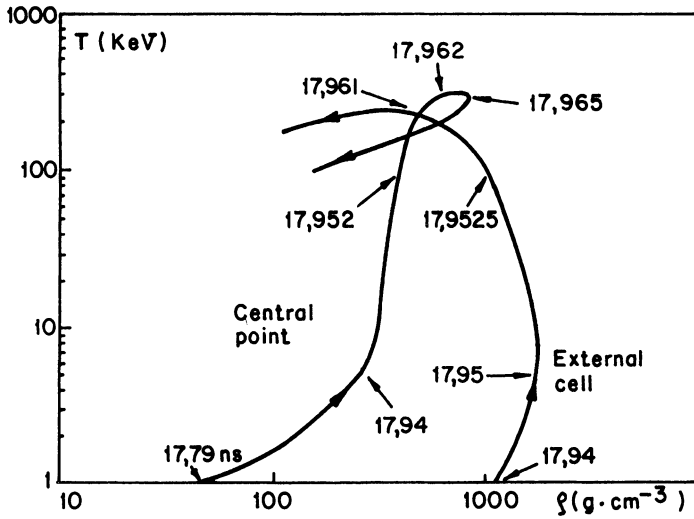


FIGURE 2 Ion temperature vs. density evolution during burnup of a target driven by 6 GeV Bi^+ ions in a 200 TW, 10 ns pulse.

by a pulse of 6 GeV at 200 TW for 10 ns. The final speed profile of the fuel is very uniform, with an average speed of 4.10^7 cm/s. The hydrodynamic efficiency is very high, close to 10%. The energy gain is 70, which is somewhat lower than the value achieved with voltage ramping in a 1 mg DT HIBALL-type target⁸ (which was 110).

4 CONCLUSIONS

Ignition conditions can be achieved with simple hollow targets driven by simple pulses of heavy ions. The dose rate delivered in the coating and the pulse length are critical parameters in order to obtain a uniform fuel acceleration. Nevertheless, the design window of successful target performances is rather large and the numerical simulation has shown that changes of 20 to 30% in magnitudes such as the beam power (maintaining the total energy) do not produce significant variations in the target gain. On the contrary, pulse specifications which produce shock waves and sudden accelerations in the innermost fuel zone lead to stagnated final states not useful to trigger ignition.

In our one-dimensional numerical simulation, instabilities have not been simulated. During the implosion process, there is a small region where $\nabla P \nabla \rho$ is negative, near the end of the ion range, but this only affects the lithium coating. In the deceleration phase after void closure, the situation can become unstable in the fuel-lithium interface, but the Atwood number is very small and the time available for instability growth is very short because ignition and burn propagation last only a few tenths of a nanosecond. Nevertheless, this issue needs further clarification to guarantee the successful performance of these targets.

REFERENCES

1. "HIBALL-II" reports UWFD-625 and KfK-3840 (1984).
2. R. D. Bangerter, W. B. Herrmannsfeldt and D. L. Judd, Editors, Lawrence Berkeley Laboratory report LBL-5543 (1976).
3. R. D. Bangerter, J. W. K. Mark and A. R. Thiessen, *Phys. Lett. A* **88**, 225 (1982).
4. G. R. Magelssen, *Nucl. Fusion* **24**, 1527 (1984).
5. N. A. Tahir, K. A. Long, *Phys. Fluids*, **30**, 1820 (1987).
6. R. D. Bangerter, *Fusion Technol.* **13**, 348 (1988).
7. G. R. Magelssen, *Fusion Technol.* **13**, 339 (1988).
8. G. Velarde *et al.*, *Nucl. Instr. Meth. Phys. Research A* **278**, 105 (1989).
9. G. Velarde *et al.*, *Atomkernenergie/Kerntechnik* **36**, 213 (1980).
10. G. Velarde *et al.*, *Atomkernenergie/Kerntechnik* **44**, 209 (1984).
11. G. Velarde *et al.*, *Laser Part. Beams* **4**, 349 (1986).
12. S. P. Ahlen, *Rev. Mod. Phys.* **52**, 121 (1980).
13. C. Yamanaka, S. Nakai, *Nature* (London) **319**, 757 (1986).
14. G. Kasotakis, L. Cicchitelli, H. Hora, *Nucl. Instr. Meth. Phys. Research A* **278**, 110 (1989).